Title

Identification of the Active Catalyst for Nickel-Catalyzed Stereospecific Kumada Coupling Reactions of Ethers

Permalink

https://escholarship.org/uc/item/7sw31760

Journal

Chemistry - A European Journal, 26(14)

ISSN

0947-6539

Authors

Dawson, David D
Oswald, Victoria F
Borovik, Andy S
et al.

Publication Date

2020-03-09

DOI

10.1002/chem.202000215

Peer reviewed

Identification of the Active Catalyst for Nickel-Catalyzed Stereospecific Kumada Coupling Reactions of Ethers

David D. Dawson[a], **Victoria F. Oswald**[a], **A. S. Borovik**[a], **Elizabeth R. Jarvo**[a]

[a]Department of Chemistry, University of California, Irvine, Irvine, CA 92697 USA

Abstract

A series of nickel complexes in varying oxidation states were evaluated as precatalysts for stereospecific cross-coupling of benzylic ethers. These results demonstrate rapid redox reactions of precatalysts, such that the oxidative state of the precatalyst does not dictate the oxidation state of the active catalyst in solution. These data provide the first experimental evidence for a Ni(0)-Ni(II) catalytic cycle for a stereospecific alkyl-alkyl cross-coupling reaction, including spectroscopic analysis of the catalyst resting state.

Graphical Abstract
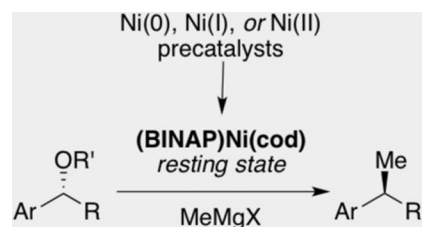
Evaluation of nickel precatalysts in different oxidation states provided evidence for active Ni(0) species in a stereospecific alkyl-alkyl cross-coupling reaction.

Keywords

nickel catalysis; precatalyst; absorption spectroscopy; cross-coupling mechanism

Nickel complexes can participate in a range of elementary reactions, including polar and single-electron events, and distinguishing mechanistic possibilities for a catalytic reaction can be challenging.[1] For many cross-coupling reactions, fundamental features of the active nickel catalyst including oxidation state have not yet been experimentally established.[2] In most nickel-catalyzed cross-coupling protocols, a Ni(0) or Ni(II) precatalyst is employed, and an active catalyst is formed in situ. The oxidation state of this active catalyst depends on several factors, and does not necessarily correspond to the oxidation state of the precatalyst.[3] Across the field, there is support for both Ni(I) and Ni(0) complexes as active catalysts, depending on the reaction details including supporting ligand and substrate. Evidence of Ni(I) complexes as active catalysts in cross-coupling reactions began with stoichiometric

erjarvo@uci.edu.

reactions of organonickel complexes. Kochi and co-workers demonstrated reductive elimination of dialkylnickel(III) complexes;[4] more recently, experimental data supporting key Ni(I) intermediates have been reported.[5,6,7,8,9,10] However, there is also evidence for catalytically active Ni(0) and Ni(II) complexes in related cross-coupling reactions,[11] including characterization of Ni(II) complexes that can enter catalytic cycles and off-cycle Ni(I) complexes.[12,13,14]

In the context of cross-coupling reactions of alkyl electrophiles, most efforts have focused on the mechanism of *stereoablative* reactions of alkyl halides. These reactions can proceed via halogen atom abstraction,[15] and Ni(I)/Ni(II)/Ni(III) catalytic cycles are typically invoked.[5,6,9] Alkyl electrophiles that undergo *stereospecific* cross-coupling, such as ethers, likely react with distinct and different mechanistic features.[16] Thus far, interrogation of these mechanisms has relied heavily on DFT calculations. In this manuscript, we present spectroscopic studies of a stereospecific Kumada coupling reaction that are consistent with a Ni(0)/Ni(II) couple (Scheme 1). We also demonstrate that both Ni(I) and Ni(II) precatalysts provide rapid entry to the catalytic cycle, underscoring the rapid redox activity of typical catalyst precursors under these reaction conditions.

We aimed to synthesize precatalysts at the Ni(0), Ni(I), and Ni(II) oxidation states that could be employed under our cross-coupling reaction conditions. The ligand in these complexes must both stabilize the nickel complexes sufficiently to provide isolable complexes, yet also allow for a reactive catalyst in our cross-coupling method. The bidentate phosphine ligand BINAP is an effective ligand in nearly all Kumada-type cross-coupling protocols disclosed by our group;[17] for this reason, it was chosen as the ligand for these experiments. The single enantiomer (*R*)-BINAP was preferentially chosen over the racemic ligand, as isolation and crystallization of enantioenriched complexes was more straightforward than the racemic analogs. Previous experiments in our laboratory have demonstrated that there are no reactivity differences or matching effects when using (*R*)-, (*S*)-, and *rac*-BINAP in Kumada cross-coupling reactions with chiral substrates.[17]

Three (*R*)-BINAP-ligated nickel precatalysts at varied oxidation states were synthesized (Scheme 2). To synthesize the Ni(0) complex **3**, a procedure by Buchwald and co-workers was employed.[18] Ni(cod)$_2$ and (*R*)-BINAP were stirred in toluene, which resulted in the clean formation of ((*R*)-BINAP)Ni(cod) as a red crystalline material (Scheme 2a). The product was recrystallized and characterized by ^{1}H & ^{31}P NMR and X-ray crystallographic analysis.[19] as well as UV-vis absorption spectroscopy, which showed a strong absorbance at λ = 535 nm.

A modified procedure by Schoenebeck was used in the synthesis of Ni(I) complex **4**.[14a] Ni(cod)$_2$ and (*R*)-BINAP were stirred in benzene to form a BINAP-ligated Ni(0) species in situ (Scheme 2b). Subsequent addition of 0.5 equivalents of chlorobenzene formed a Ni(II) species by an oxidative addition pathway, which allowed for a comproportionation reaction between Ni(0) and Ni(II) species. The reaction afforded the paramagnetic ((*R*)-BINAP)NiCl, which was crystallized. Due to the open coordination site on the Ni(I) center, ((*R*)-BINAP)NiCl crystallizes as a dimer with pseudo-tetrahedral geometry.[20] In solution, however, the complex is monomeric; the EPR spectrum shows an expected strong signal.

Finally, Ni(II) complex **5** was synthesized according to the procedure reported by Jamison and co-workers.[18, 21, 22] $NiCl_2 \cdot 6H_2O$ was refluxed with (*R*)-BINAP in acetonitrile (Scheme 2c). The resultant black solid was recrystallized, which afforded ((*R*)-BINAP)$NiCl_2$ as sparingly soluble black crystals.[22] Crystallographic analysis confirmed pseudo-square planar geometry around the nickel center.[23] This pseudo-square planar geometry combined with its low solubility in most common solvents made additional characterization of the Ni(II) species difficult. However, the ^{1}H NMR spectrum correlated with related complexes reported in the literature,[24] and the magnetic moment was measured to be 2.49 μ_B by Evan's Method,[25] consistent with the assigned structure.

With nickel complexes **3**–**5** in hand, we examined them as catalysts in a cross-coupling reaction of a benzylic ether. We chose cross-coupling of tetrahydropyran **6** with methylmagnesium iodide, a prototypical stereospecific Kumada-type coupling reaction that is robust, high-yielding, and scales well (Figure 1a).[26] The active catalyst is proposed to be either Ni(0) or Ni(I) species ligated by the bidentate phosphine ligand; under typical reaction conditions the precatalyst would undergo reduction and oxidation pathways in situ to generate the active catalyst. Figure 1 shows a comparison of the rate of product formation with ((*R*)-BINAP)Ni(cod) (blue diamonds), ((*R*)-BINAP)NiCl (pink squares), and ((*R*)-BINAP)$NiCl_2$ (orange triangles).

Comparison of the rate profiles using Ni(I) precatalyst **4** (pink squares) and Ni(II) precatalyst **5** (orange triangles) show that both form products with similar rates throughout the 6 hour window (Figure 1b). This observation is consistent with rapid reduction of both complexes with the Grignard reagent to generate the same active catalyst in solution. The slightly lower initial rate with Ni(II) precatalyst **5** can be attributed to slightly slower reduction of **5** by the Grignard reagent (vide infra, Figure 2b and c).

In contrast, Ni(0) precatalyst **3** provided substantially suppressed rate of product formation when compared to Ni(I) and Ni(II) catalysts **4** and **5** (Figure 1b, blue diamonds). We reasoned that this was due to inhibition by cod by formation of a stable off-cycle species. To determine whether or not cod suppresses the rate of reaction, 5 mol % of cod was added to the reactions employing ((*R*)-BINAP)NiCl and ((*R*)-BINAP)$NiCl_2$ (Figure 1c). With cod present in all reactions, the rates of formation of product **7** using Ni(I) and Ni(II) are slowed, and are similar to the rate using the Ni(0) precatalyst. These observations are consistent with formation of the same catalyst resting state, e.g., (BINAP)Ni(cod), from all three precatalysts.

As shown above, coordination of cod to nickel species clearly retards reaction progress, likely by stabilizing an off-cycle nickel complex. Although this adversely affects the rate of product formation, it could also slow or prevent catalyst decomposition by reaction with Grignard reagent. To test this hypothesis, nickel precatalysts were allowed to stir with Grignard reagent for two hours prior to addition of substrate (Figure 1d). Surprisingly, upon addition of ether **6**, no product formation was seen for either the Ni(I) or Ni(II) catalyst, even at six hours. This lack of product formation is likely caused by reaction of the nickel complexes with the Grignard reagent, which results in reduction and formation of nickel black. In contrast, the Ni(0) catalyst ((*R*)-BINAP)Ni(cod) is stabilized and protected by the

cod ligand during the two hour prestir with Grignard reagent; upon addition of substrate, product formation is comparable to that observed without the two hour prestir. This experiment highlights the ability of cyclooctadiene to stabilize low valent nickel complexes and protect from catalyst degradation. For applications where a robust catalyst is required such as large scale applications, use of a cod-ligated precatalyst would provide a protective effect.

To provide evidence as to the exact structure of the active catalyst, including whether the oxidation state of the resting state complex is Ni(0) or Ni(I), we undertook spectroscopic tests to further characterize nickel complexes that are present in situ. There are many spectroscopic techniques that are regularly employed to analyze organometallic complexes, but due to the electronic properties and coordination geometry of these nickel compounds, absorption spectra proved most informative.

We characterized each precatalyst using absorption spectra (Figure 2a), and then compared to spectra of Kumada reactions employing each catalyst. As shown in Figure 2a, **3** displayed a distinctive absorption at $\lambda_{max} = 535$ nm, whereas the spectra for Ni(I) and Ni(II) complexes **4** and **5** featured a series of peaks of lower intensity.[22] Addition of substrate to each of the preformed catalysts did not alter the absorption spectra.[27] Upon the addition of Grignard reagent, there is no change in signal for the solution of **3**,[27] which is consistent with the unchanged catalytic activity of the Ni(0) catalyst upon stirring with Grignard reagent (*c.f.* Figure 1d). In contrast, the Ni(I) and Ni(II) spectra changed drastically upon addition of Grignard reagent, with disappearance of most identifiable peaks (Figure 2b and 2c). These results, in conjunction with lack of product formation from these mixtures (Figure 1d), are consistent with reduction and decomposition of **4** and **5** by the Grignard reagent to form inactive complexes. We sought corroborate this premise using electron paramagnetic resonance (EPR) spectroscopy. Upon addition of Grignard reagent to complex **4**, the strong Ni(I) signal ($g = 2.13$) is immediately quenched, consistent with the formation of an even electron species. Even-electron complexes **3** and **5** were EPR silent and showed no signal after addition of the Grignard reagent to the EPR tube.[27]

These absorption spectra, combined with reaction rate data, are consistent with the Grignard reagent affecting a transformation of the precatalysts in situ, generating an even electron species. Considering our previous results that show the stabilizing effect of the cod ligand in the reaction, we anticipated that adding an equivalent of cod to the Ni(I) and Ni(II) solutions might produce a more stable complex. Thus, solutions of Ni(I) complex **4** and Ni(II) complex **5** were treated with Grignard reagent in the presence of cod and analyzed by absorption spectroscopy. The results show the influence of cod on the reaction (Figure 2d and 2e): after two hours, both Ni(I) and Ni(II) complexes in the presence of cod converged on the same intense spectrum with an intense signal that was previously observed with Ni(0) complex **3**, with a strong absobance at $\lambda_{max} = 535$ nm. These results are consistent with a pathway where upon addition of Grignard reagent, Ni(I) and Ni(II) species are rapidly reduced to Ni(0) (Figure 2f), at which point they are stabilized by the cod ligand to generate the same complex, (BINAP)Ni(cod). The lack of a substantial induction period in the cross-coupling rates employing Ni(I) and Ni(II) complexes is likely because of the rapid redox activity of these complexes that leads to rapid reduction to Ni(0).

Based on the results of these experiments we propose that, in the absence of cod, the active catalyst is arene-ligated complex **8**. In the presence of cod, the stable off-cycle (BINAP)Ni(cod) species **3** is formed; upon ligand exchange with substrate the catalyst can enter the catalytic cycle. In reactions that utilize Ni(I) or Ni(II) catalysts **4** or **5**, immediate reduction by MeMgI forms the on-cycle active catalyst **8**. This proposed reduction pathway is supported by the results in Figure 2b–e and EPR studies, which indicated an instantaneous reaction between the precatalysts and MeMgI, and that resulted in a substantial changes in the absorbance spectra, loss of the Ni(I) EPR signal indicating formation of even-electron species. When no substrate or cod is present (as in Figure 1d), the low valent nickel complexes decompose, likely generating nickel black. However, when cod is present, low-valent complexes can be stabilized by forming off-cycle resting state **3**; this resting state is observed by absorption spectroscopy (Figure 2d–e). These conclusions are consistent with the results of our prior investigations of the mechanism of nickel-catalyzed coupling of benzylic ethers, including DFT calculations of the reaction coordinate diagram for the catalytic cycle.[16a]

Conclusions

Our spectroscopic studies have provided clarity on the identity of the active catalyst of our nickel-catalyzed Kumada-type cross-coupling reaction. The use of preformed nickel catalysts allowed us to probe the effect of varying nickel oxidation states as it relates to catalytic activity. Two components of our reaction manifold, the 1,5-cyclooctadiene ligand (cod) and Grignard reagent (MeMgI), were found to have a dramatic influence. Addition of MeMgI to solutions containing Ni(I) and Ni(II) preformed catalysts resulted in a rapid reaction that altered the oxidation state of the catalytic precursor. The presence of cod provided a stabilizing effect on the catalyst, protecting it from MeMgI induced decomposition, yet also mildly supressing the rate of the cross-coupling reaction. When solutions of Ni(I) and Ni(II) containing exogenous cod were subjected to MeMgI, absorption spectra confirmed convergence on a single species, which matched that of ((R)-BINAP)Ni(cod). These data, combined with the absence of single-electron species in the EPR spectra, provide experimental evidence that the stereospecific Kumada-type cross-coupling reaction proceeds via a Ni(0)/Ni(II) catalytic cycle. In contrast, stereoablative alkyl-alkyl cross-coupling reactions are typically proposed to involve Ni(I) intermediates.

Supplementary Material

Refer to Web version on PubMed Central for supplementary material.

Acknowledgements

References

1. (a)Hartwig JH, Organotransition Metal Chemistry: From Bonding to Catalysis, 1st ed.; University Science Books: Sausalito, California, 2010.(b)Modern Organonickel Chemistry, 1st ed.; Tamaru Y, Ed.; Wiley-VCH John Wiley & Sons, Inc.: Hoboken, New Jersey, 2005.

2. (a)Tasker SZ, Standley EA, Jamison TF, Nature, 2014, 509, 299–309. [PubMed: 24828188] (b)Cherney AH, Kadunce NT, Reisman SE, Chem. Rev 2015, 115, 9587–9652. [PubMed: 26268813]

3. For a discussion, see: Jahn U, Top. Curr. Chem 2012, 320, 323. [PubMed: 22143611]

4. (a)Morrell DG, Kochi JK, J. Am. Chem. Soc 1975, 97, 7262–7270.(b)Tsou TT, Kochi JK, J. Am. Chem. Soc 1979, 101, 7547–7560.

5. (a)Anderson TJ, Jones GD, Vicic DA, J. Am. Chem. Soc 2004, 126, 8100–8101. [PubMed: 15225035] (b)Jones GD, McFarland C, Anderson TJ, Vicic DA, Chem. Commun 2005, 4211–4213.

6. Zultanski SL, Fu GC, J. Am. Chem. Soc 2011, 133, 15362–15364. [PubMed: 21913638]

7. Biswas S, Weix DJ, J. Am. Chem. Soc 2013, 135, 16192–16197. [PubMed: 23952217]

8. Cornella J, Gomez-Bengoa E, Martin R, J. Am. Chem. Soc 2013, 135, 1997–2009. [PubMed: 23316793]

9. Breitenfeld J, Ruiz J, Wodrich MD, Hu X, J. Am. Chem. Soc 2013, 135, 12004–12012. [PubMed: 23865460]

10. Yin H, Fu GC, J. Am. Chem. Soc 2019, 141, 15433–15440. [PubMed: 31502449]

11. Quasdorf KW, Antoft-Finch A, Liu P, Silberstein AL, Komaromi A, Blackburn T, Ramgren SD, Houk KN, Snieckus V, Garg NK, J. Am. Chem. Soc 2011, 133, 6352–6363. [PubMed: 21456551]

12. a)Huang C-Y, Doyle AG, J. Am. Chem. Soc 2012, 134, 9541–9544. [PubMed: 22414150] b)Maity P, Shacklady-McAtee DM, Yap GPA, Sirianni ER, Watson MP, J. Am. Chem. Soc 2012, 135, 280–285. [PubMed: 23268734]

13. (a)Guard LM, Mohadjer-Beromi M, Brudvig GW, Hazari N, Vinyard DJ, Angew. Chem. Int. Ed, 2015, 54, 13352–13356.(b)Beromi MM, Nova A, Balcells D, Brasacchio AM, Brudvig GW, Guard LM, Hazari N, Vinyard DJ, J. Am. Chem. Soc 2017, 139, 922–936. [PubMed: 28009513]

14. (a)Yin G, Kalvet I, Englert U, Schoenebeck F, J. Am. Chem. Soc 2015, 137, 4164–4172. [PubMed: 25790253] (b)Ge S, Green RA, Hartwig JF, J. Am. Chem. Soc 2014, 136, 1617–1627. [PubMed: 24397570]

15. (a)Kehoe R, Mahadevan M, Manzoor A, McMurray G, Wiendefeld P, Baird MC, Budzelaar PHM, Organometallics 2018, 37, 2450–2467.(b)Diccianni JB, Katigbak J, Hu C, Diao T, J. Am. Chem. Soc 2019, 141, 1788–1796. [PubMed: 30612428]

16. (a)Chen P-P, Lucas EL, Greene MA, Zhang S-Q, Tollefson EJ, Erickson LW, Taylor BLH, Jarvo ER, Hong X, J. Am. Chem. Soc 2019, 141, 5835–5855. [PubMed: 30866626] (b)Zhang S-Q, Taylor BLH, Ji C-L, Gao Y, Harris MR, Hanna LE, Jarvo ER, Houk KN, Hong X, J. Am. Chem. Soc 2017, 139, 12994. [PubMed: 28838241]

17. (a)Taylor BLH, Swift EC, Waetzig JD, Jarvo ER, J. Am. Chem. Soc 2011, 133, 389–391. [PubMed: 21155567] (b)Taylor BLH, Harris MR, Jarvo ER, Angew. Chem. Int. Ed 2012, 51, 7790–7793.(c)Greene MA, Yonova IM, Williams FJ, Jarvo ER, Org. Lett 2012, 14, 4293–4296. [PubMed: 22568515] (e)Tollefson EJ, Dawson DD, Osborne CA, Jarvo ER, J. Am. Chem. Soc. 2014, 136, 14951–14958. [PubMed: 25308512]

18. Spielvogel DJ, Davis WM, Buchwald SL, Organometallics 2002, 21, 3833–3836.

19. CCDC 1569388.

20. CCDC 1569387.

21. Standley EA, Smith SJ, Muller P, Jamison TF, Organometallics 2014, 33, 2012–2018. [PubMed: 24803717]

22. Vogler A, Inorg. Chem. Comm 2016, 65, 39–40.

23. CCDC 1569386.

24. For ^{1}H NMR spectra of related complexes:Ni((*S*)-BINAP)]Br$_2$: reference 18;[Ni((*S*)-Tol-BINAP)]Cl$_2$:Evans DA, Thomson RJ, Franco F, J. Am. Chem. Soc 2005, 127, 10816–10817. [PubMed: 16076172]

25. Evans DF, J. Chem. Soc 1959, 2003–2005.

26. Dawson DD, Jarvo ER, Org. Proc. Res. Dev 2015, 19, 1356–1359.

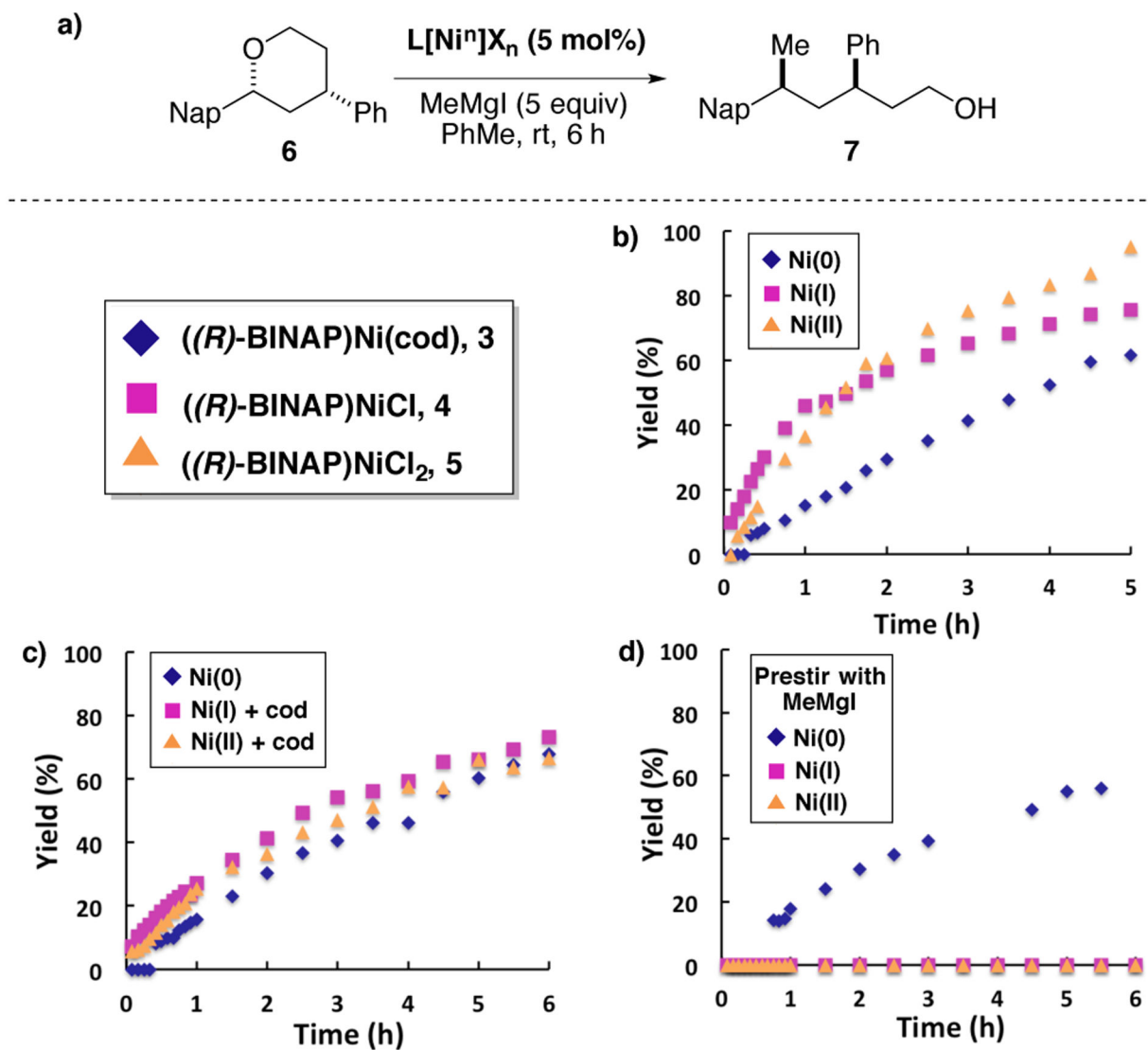27. See Supporting Information for full details.

Figure 1.
Relative rate experiments: a) Cross-coupling of **6**. b) Formation of product **7** over time using ((*R*)-BINAP)Ni(cod) (blue), ((*R*)-BINAP)NiCl (pink), and ((*R*)-BINAP)NiCl$_2$ (orange); c) Formation of product **7** over time in the presence of cyclooctadiene: ((*R*)-BINAP)Ni(cod) (blue); ((*R*)-BINAP)NiCl + 0.05 equiv cod (pink); and ((*R*)-BINAP)NiCl$_2$ + 0.05 equiv cod (orange); d) Formation of product **7** over time after a 2 hour pre-stir of precatalyst with MeMgI, followed by addition of substrate **6**: ((*R*)-BINAP)Ni(cod) (blue); ((*R*)-BINAP)NiCl (pink); and ((*R*)-BINAP)NiCl$_2$ (orange). See Supporting Information for full details.
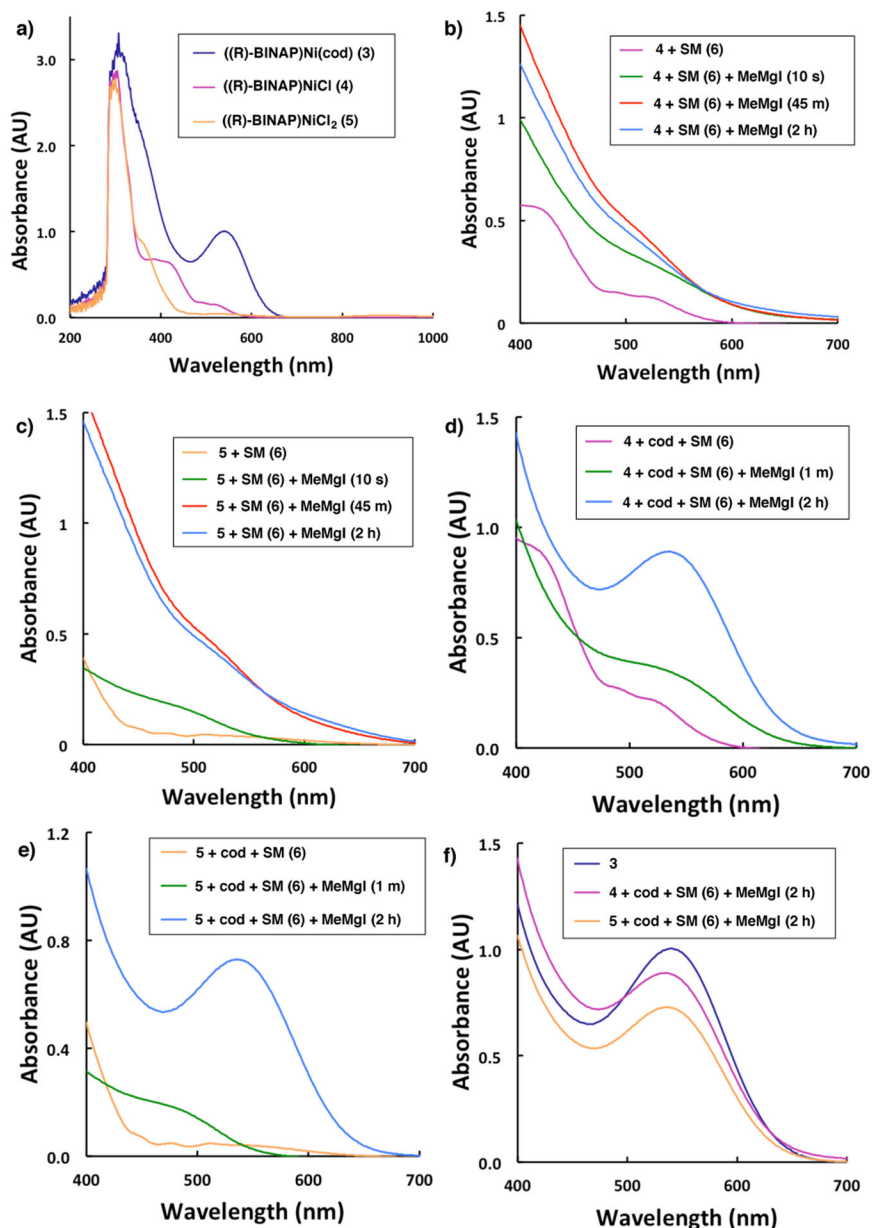
Figure 2.
Kumada reactions employing 5 mol% of precatalysts **3**-**5**, monitored by absorption spectroscopy. a) Absorbance spectra for complexes ((*R*)-BINAP)Ni(cod) (blue), ((*R*)-BINAP)NiCl (pink), and ((*R*)-BINAP)NiCl$_2$ (orange); b) Addition of MeMgI to ((*R*)-BINAP)NiCl; c) Addition of MeMgI to ((*R*)-BINAP)NiCl$_2$; d) Addition of MeMgI to ((*R*)-BINAP)NiCl + 0.05 equiv cod; e) Addition of MeMgI to ((*R*)-BINAP)NiCl$_2$ + 0.05 equiv cod; f) comparison to ((*R*)-BINAP)Ni(cod).
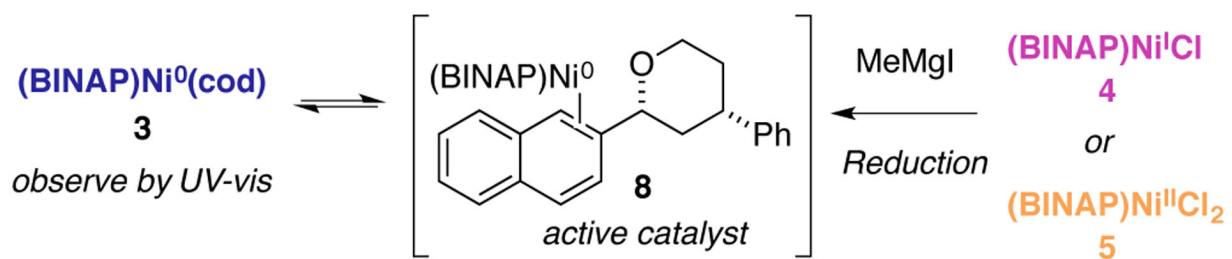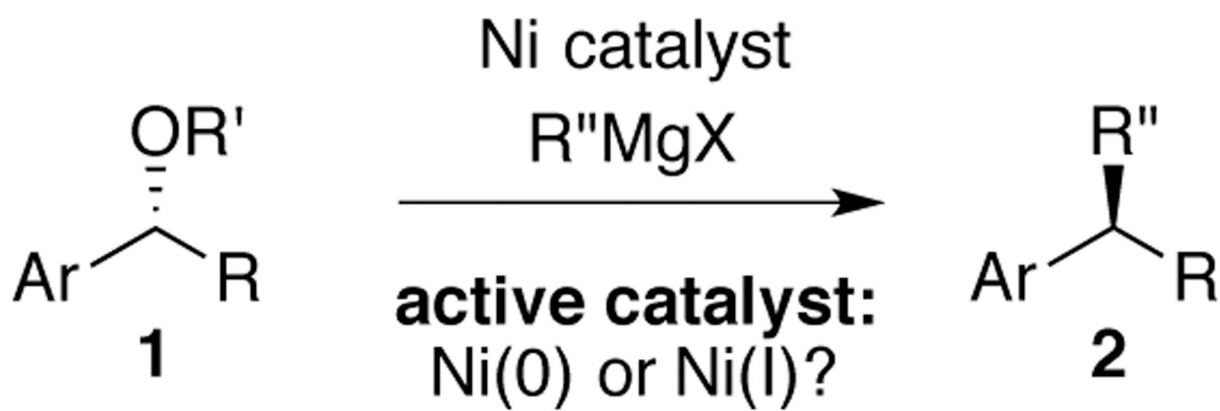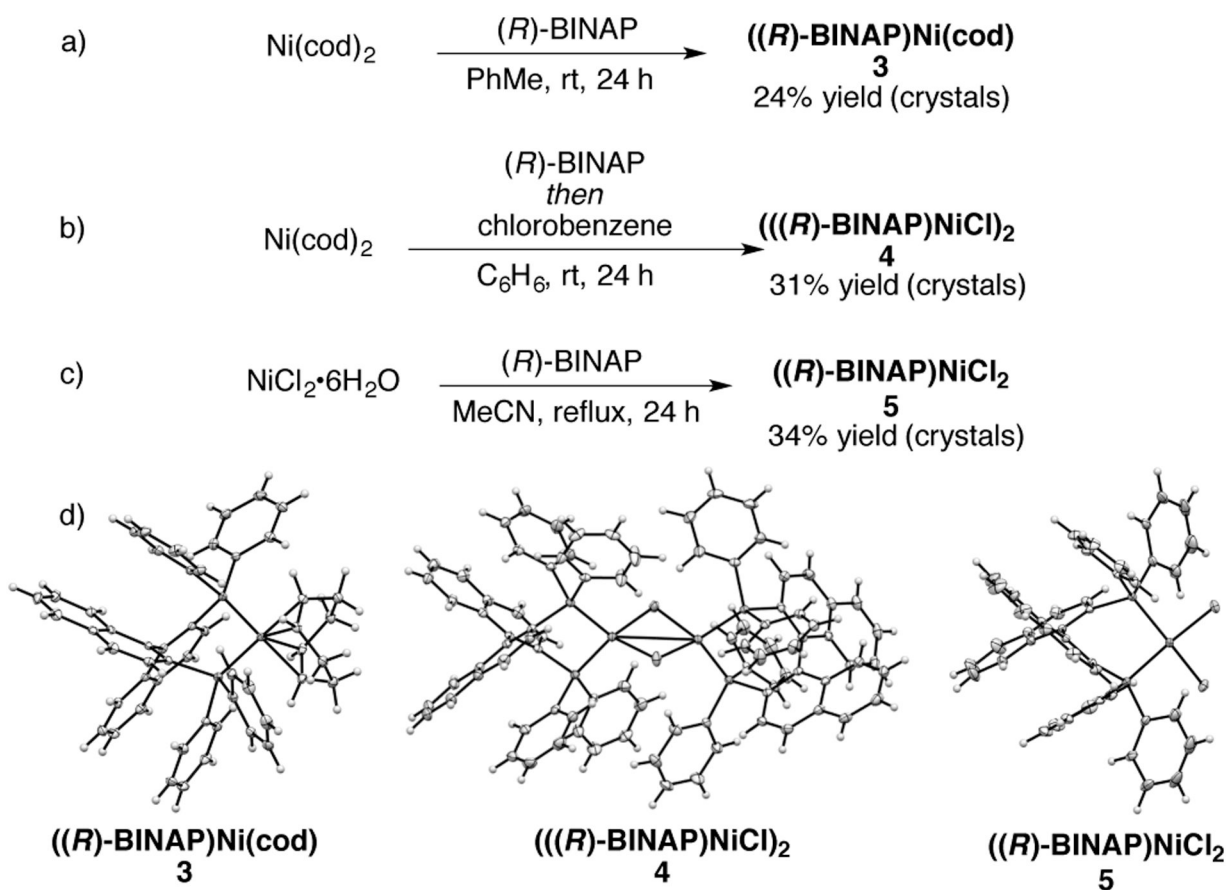
Figure 3.
Mechanistic hypothesis.

Scheme 1.
Nickel-catalyzed stereospecific Kumada cross-coupling.

a) $Ni(cod)_2$ $\xrightarrow[\text{PhMe, rt, 24 h}]{(R)\text{-BINAP}}$ **((R)-BINAP)Ni(cod)**
3
24% yield (crystals)

b) $Ni(cod)_2$ $\xrightarrow[\text{C}_6\text{H}_6\text{, rt, 24 h}]{\substack{(R)\text{-BINAP} \\ then \\ \text{chlorobenzene}}}$ **(((R)-BINAP)NiCl)$_2$**
4
31% yield (crystals)

c) $NiCl_2 \cdot 6H_2O$ $\xrightarrow[\text{MeCN, reflux, 24 h}]{(R)\text{-BINAP}}$ **((R)-BINAP)NiCl$_2$**
5
34% yield (crystals)

d)

((R)-BINAP)Ni(cod)
3

(((R)-BINAP)NiCl)$_2$
4

((R)-BINAP)NiCl$_2$
5

Scheme 2.
Synthesis and key characterization data for precatalysts.